Journal of Catalysis 270 (2010) 310–317

Contents lists available at ScienceDirect

Journal of Catalysis

journal homepage: www.elsevier.com/locate/jcat

Selective catalytic oxidation of ammonia to nitrogen over mesoporous CuO/RuO_2 synthesized by co-nanocasting-replication method

Xiangzhi Cui, Jian Zhou, Zhengqing Ye, Hangrong Chen, Lei Li, Meiling Ruan, Jianlin Shi *

State Key Laboratory of High Performance Ceramics and Superfine Microstructure, Shanghai Institute of Ceramics, Chinese Academy of Sciences, Shanghai 200050, PR China

ARTICLE INFO

Article history:
Received 30 October 2009
Revised 4 January 2010
Accepted 6 January 2010
Available online 6 February 2010

Keywords:
Mesoporous
Copper–ruthenium bimetal oxide
Ammonia oxidation
Selectivity

ABSTRACT

A new type of catalyst for ammonia selective catalytic oxidation, mesoporous CuO/RuO_2 with well-crystallized framework and ordered mesoporous structure, has been synthesized by a co-nanocasting-replication method. Various techniques have been employed for the material characterization. The prepared mesostructured bimetal oxides demonstrated high catalytic activity and N_2 selectivity toward NH_3 oxidation reaction in the presence of excess oxygen. The temperature for the complete ammonia oxidation was as low as 180 °C on the mesoporous 10 wt.% CuO/RuO_2 composite, and there was no apparent decrease in the catalytic activity at prolonged reaction time. Both high ammonia conversion up to 100% and high N_2 selectivity (>95%) were achieved on the mesoporous 5–15 wt.% CuO/RuO_2 composites. A synergetic catalytic mechanism between copper and ruthenium component was proposed to understand the promoted catalytic effect, especially the achievement of both high conversion and high selectivity for N_2 by CuO.

1. Introduction

The increasing problem of air pollution by N-containing compounds, such as NO, NO_2, N_2O and NH_3, has led to more and more stringent emission control. The removal of ammonia from waste streams is becoming an increasingly important issue. It is known that many chemical processes use reactants containing ammonia or produce ammonia as a by-product. The selective catalytic oxidation (SCO) of ammonia to nitrogen and water is one of the best potential approaches nowadays for removing ammonia from oxygen-containing waste gases, and consequently it has become of increasing interest in recent years [1–5]. The oxidation of ammonia can proceed via the following principal reactions [6]:

$$4NH_3 + 5O_2 = 4NO + 6H_2O \quad (1)$$

$$4NH_3 + 3O_2 = 2N_2 + 6H_2O \quad (2)$$

The process described in reaction (2) is a potentially effective and technologically important method to eliminate ammonia pollution, and it is becoming the most promising method for cleaning of large gas flows containing oxygen and ammonia [1,7]. This method can be applied for the treatment of waste gases emitted from chemical processes in which ammonia is used as a reactant or produced as a by-product.

Various types of materials have been studied as catalysts for ammonia SCO reaction. Noble metals including Pt [8,9], Pd [8,10], Ru [10], Ir [11], Ag [11,12] have been found to be very active catalysts for the ammonia oxidation. Ammonia oxidation reactions catalyzed by these noble metal catalysts proceed at relatively low temperature, for example, the NH_3 oxidation temperatures on Al_2O_3 or ZSM-5 supported Pd, Rh and Pt catalysts were at 200–350 °C. However, the selectivities for N_2, i.e., SCO of NH_3 to N_2 on these catalysts are relatively low (typically ⩽80%). The next group of catalysts for the ammonia SCO process is based on transition metal oxides, such as MnO_2, Co_3O_4, Fe_2O_3, CuO, MoO_3, V_2O_5 [13–19]. These catalysts showed higher N_2 selectivity; however, they needed significantly higher operation temperatures (300–400 °C) than the noble metal catalysts. Recently developed catalysts were aimed to combine the advantages of earlier two types of catalysts, to enhance both the catalytic activity and the N_2 selectivity for NH_3 oxidation. This group catalysts included Fe-exchanged zeolites (Fe-ZSM-5) [4,5], Fe-exchanged zeolites supported noble metals (Pt, Pd, Rh) [10], and activated carbon fiber (ACF) supported copper catalyst [20], which showed 95–97% NH_3 conversion and 97–100% N_2 selectivity for ammonia SCO reaction. Though V_2O_5/TiO_2 catalyst reported by Li and Armor [21] was quite selective for N_2 at $T < 300$ °C; however, it was much less active compared to the precious metal catalysts for NH_3 oxidation at 200–350 °C. Lu et al. [22] presented that the alumina supported copper-based catalyst ($CuAl_2O_4$-like) was more active than CuO for the ammonia oxidation reaction. Recently, Hung [23] found that the Cu:La molar ratio in the CuO/La_2O_3 bimetal oxide catalyst had great effect on the ammonia catalytic oxidation at temperatures from 150 to

* Corresponding author. Fax: +86 21 52413122.
E-mail addresses: jlshi@sunm.shcnc.ac.cn, jlshi@mail.sic.ac.cn (J. Shi).

0021-9517/$ - see front matter © 2010 Elsevier Inc. All rights reserved.
doi:10.1016/j.jcat.2010.01.005

500 °C in the presence of oxygen. As a whole, however, it is still a great challenge to achieve both complete ammonia conversion at relatively low temperature and high N_2 selectivity of ammonia oxidation by using low cost catalysts.

It is well known that mesoporous materials are a new group of porous materials and very attractive for their potential catalytic applications, which are characterized by ordered pore structure, large surface area, porosity and high thermal stability [24–27]. However, there is no report about using mesoporous bimetal oxide as catalyst for the ammonia SCO as far as we know, though non-mesoporous V_2O_5/TiO_2 and CuO/La_2O_3 bimetal oxide catalysts have been reported [21,23]. Previously, we reported that a high surface area mesoporous hydrous ruthenium oxide (RuO_xH_y) prepared at 350 °C showed high electrochemical catalytic activity due to its special mesoporous structure [28]. In this report, we aim to prepare mesoporous CuO/RuO_2 bimetal oxides and use them as the ammonia SCO catalysts and try to achieve complete ammonia conversion at relative low temperatures and meanwhile high selectivity of ammonia oxidation to nitrogen. The catalysts were prepared by a co-nanocasting-replication method using mesoporous silica (KIT-6) as hard template, and the mesostructured bimetal oxides showed a 100% ammonia conversion and near 98% N_2 selectivity at a temperature as low as 180 °C. A synergetic catalytic effect between RuO_2 and CuO has been proposed to understand the catalytic performance.

2. Experimental

2.1. Synthesis of mesoporous silica (KIT-6)

The mesoporous silica (KIT-6) with cubic *Ia*3*d* symmetry was prepared according to the published procedure [29] with minor modification. Typically, 6 g of surfactant P_{123} and 6 g of *n*-butanol were dissolved in a HCl solution, which was prepared by mixing 11.4 g of concd. HCl (37 wt.%) in 217 g distilled water. To this homogeneous solution, 12.9 g of tetraethylorthosilicate (TEOS) was added and continuously stirred for 24 h at 38 °C, which was slightly higher than the reported (35 °C) procedure [29]. Then, the mixture was transferred to teflon-lined autoclave and heated at 100 °C for another 24 h. The solid product was filtered, washed with distilled water and calcined at 550 °C for 5 h to remove the organic template.

2.2. Preparation of mesoporous CuO/RuO_2 bimetal oxides

Mesoporous RuO_2 and CuO/RuO_2 materials were prepared by a one-step co-nanocasting method using KIT-6 as hard template. A mixed solution of Cu(II) nitrate and Ru (III) chloride (totally 0.8 g) was prepared by dissolving $Cu(NO_3)_2{\cdot}3H_2O$ and $RuCl_3$ in 2 mL ethanol. The weight percentage *X* of Cu(II) oxide (CuO) in the bimetal oxide, $X = ([CuO]/([CuO] + [RuO_2])) \times 100$, was varied from 5 to 30. The prepared mesoporous copper–ruthenium bimetal oxides were named as *X*-CuO/RuO_2. Typically, 2 mL of previously prepared ethanol solution including copper and ruthenium precursors was co-impregnated into 0.4 g of KIT-6 template. After the ethanol was evaporated, the ruthenium–copper/silica composite was kept under ammonia vapor for 24 h at room temperature to convert the ruthenium precursor into metal hydroxide. After that, the obtained composite was calcined at 500 °C for 3 h. The silica template was finally removed by treating in a 2 M heated (90 °C) NaOH solution. The template-free products were collected by centrifugation, washed with distilled water, dried at room temperature in vacuum and named as m-RuO_2 (0-CuO/RuO_2), 5-CuO/RuO_2, 10-CuO/RuO_2, 15-CuO/RuO_2, 20-CuO/RuO_2 and 30-CuO/RuO_2 according to the amount of CuO addition.

2.3. Material characterization

The powder X-ray diffraction (XRD) patterns of prepared samples were recorded on a Rigaku D/Max-2550V X-ray diffractometer with a Cu Kα radiation target (40 kV, 40 mA). The scanning rates were 0.6°/min and 6°/min for the low-angle and wide-angle XRD measurements, respectively. The N_2 sorption measurement was performed using Micromeritics Tristar 3000 at 77 K, and the specific surface area and the pore size distribution were calculated using the Brunauer–Emmett–Teller (BET) and Barrett–Joyner–Halenda (BJH) methods, respectively. Transmission electron microscopy (TEM) images were obtained on a JEOL 200CX electron microscope operating at 160 kV. Energy-dispersive X-ray (EDX) spectra were collected from a JEM-2010 electron microscope operated at 200 kV. X-ray photoelectron spectroscopy (XPS) signals were collected on a VG Micro MK II instrument using monochromatic Mg Kα X-rays at 1253.6 eV operated at 150 W, and spectrum calibration was performed by taking the C 1s electron peak (BE = 285 eV) as internal reference.

2.4. Catalytic tests

The catalytic reactions for ammonia SCO were carried out under atmospheric pressure in a temperature-programmed reaction, fixed-bed quartz–glass reactor (6.0 mm in inner diameter) using a thermal conductivity detector (TCD) of a gas chromatograph

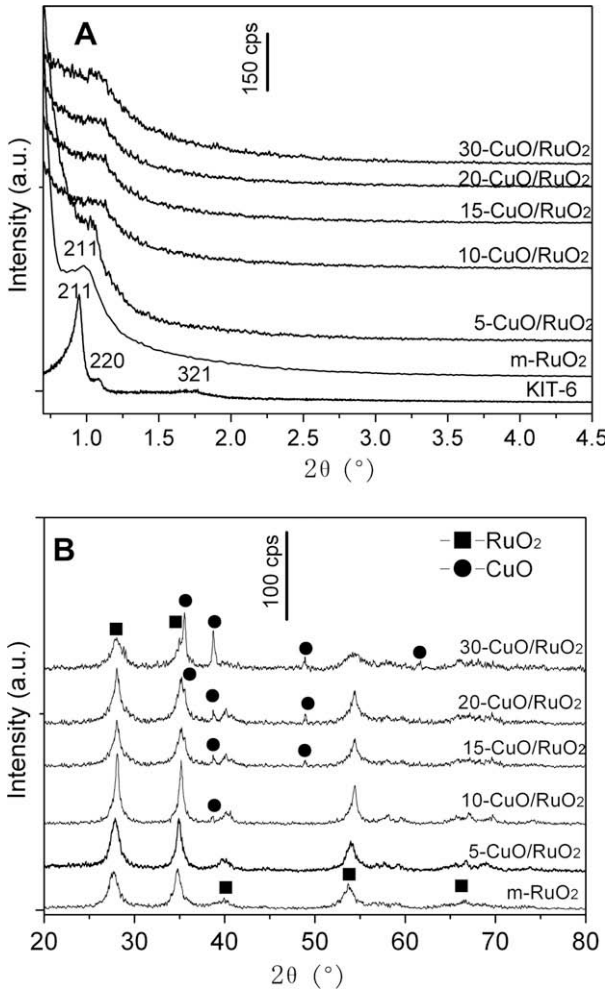

Fig. 1. Small-angle (A) and wide-angle (B) XRD patterns for the prepared mesoporous RuO_2 and CuO/RuO_2 composites.

(HP 6890 series GC system). The reactant gas was obtained by blending different gas flows, and the typical reactant gas composition was as follows: 1000 ppm NH_3, 2% O_2 and balance He. The total flow rate was 100 mL min^{-1} (at ambient temperature and pressure), and a space velocity of 75,000 mL h^{-1} $gcat^{-1}$ was obtained. In a typical reaction, 80 mg catalyst was supported on the quartz cotton in a quartz–glass tube reactor and thermally treated from room temperature to 350 °C at 6 °C min^{-1}. The concentration of the outlet NH_3 after stepwise changes in the reaction temperature was analyzed with an on-line gas chromatograph (SP-6890, molecular sieves 13×column) equipped with a TCD. Multiple concentrations of the outlet gas were taken and averaged to ensure that the catalytic system had reached a steady state. The conversion of NH_3 was calculated using the integrated peak area differences between the initially fed NH_3 and the effluent NH_3 from the reactor with an accuracy of about ±5%.

3. Results and discussion

3.1. Characterization of prepared samples

Fig. 1A gives the low-angle XRD patterns of the prepared silica-free replicas. All samples showed characteristic reflections of

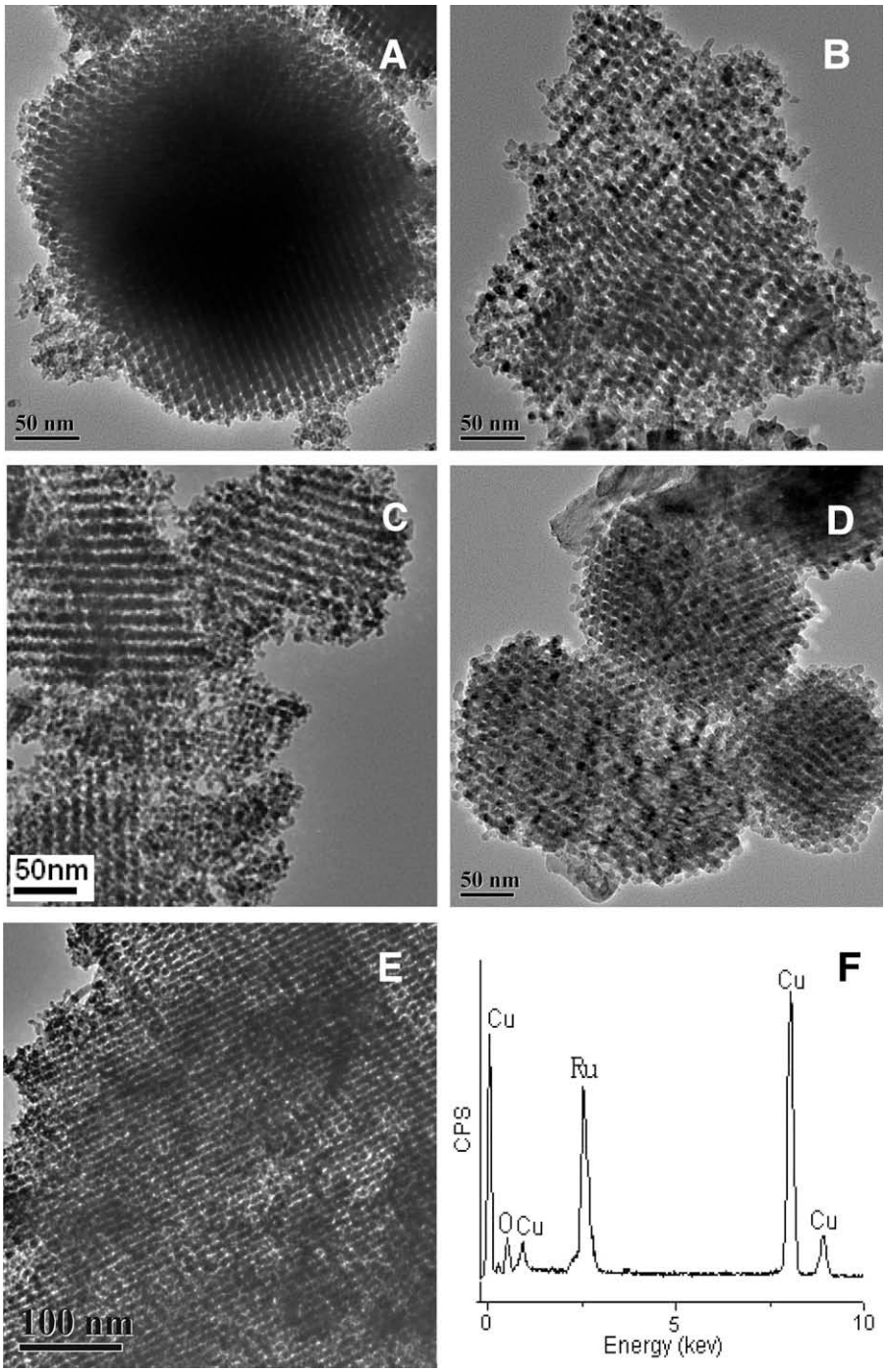

Fig. 2. TEM images of prepared samples of (A) m-RuO_2, (B) 10-CuO/RuO_2, (C) 15-CuO/RuO_2, (D) 20-CuO/RuO_2 and (E) 30-CuO/RuO_2; and EDX spectrum (F) of mesoporous RuO_2.

(2 1 1) planes at 2θ value of about 1°, corresponding to the main (2 1 1) diffraction peak of the cubic *Ia*3*d* symmetry of mesoporous silica template, though their positions had shifted toward higher angles. However, only (2 1 1) reflections were observable for all the replicas, and they were relatively broad and low in intensity, suggesting that the mesostructures of prepared RuO_2 or CuO/RuO_2 composites were less ordered than their silica template. The wide-angle XRD patterns of the prepared replicas are shown in Fig. 1B. For samples with copper oxide contents of 0–5 wt.%, the diffraction patterns are quite similar, and all the Bragg diffraction peaks can be indexed to ruthenium dioxide (RuO_2, JCPDS 65-2824), and the diffraction peaks of CuO can hardly be found. However, weak diffraction peaks of tenorite (CuO) could be identified in 10-CuO/RuO_2, and the intensity of it became stronger with the increase in CuO content for samples 15-CuO/RuO_2, 20-CuO/RuO_2 and 30-CuO/RuO_2. In addition, the broadened diffraction peaks of all the replicas indicated that the crystallites were nano-sized because of the effectively restrained growth of crystalline particles by the framework of silica template during calcination. The mesostructure of the silica template played a role of a micro-reactor for the formation of nano-sized CuO/RuO_2 structure during the synthesis procedure.

The typical TEM images of the prepared samples are shown in Fig. 2. The ordered arrangement of the mesoporous m-RuO_2 can be clearly observed in [1 0 0] direction (Fig. 2A). Fig. 2B–E is the TEM images of 10-CuO/RuO_2, 15-CuO/RuO_2, 20-CuO/RuO_2 and 30-CuO/RuO_2 replica in the view of [3 1 1], [1 1 0], [1 1 0] and [1 1 1], respectively, indicating that the ordered pore structure of copper–ruthenium bimetal oxides has been well or partially retained. In addition to the ordered areas in the images, the disordered regions among them, such as those in Fig. 2C, could also be found suggesting the partial collapse of the mesopores. This was probably resulted from the incomplete CuO/RuO_2 filling into the pore channels due to the volume shrinkage by the precursor decomposition during calcination and thus structural collapse during dissolution of the silica template. This was also in agreement with the result of low-angle XRD pattern where they showed only one characteristic diffraction peak of the cubic mesoporous structure. No other signals such as silica or sodium, except for Ru and Cu, were detected in sample 10-CuO/RuO_2 according to the EDX spectrum in Fig. 2F, indicating the complete removal of the silica template by heated NaOH solution.

The surface compositional information of the prepared CuO/RuO_2 composite was collected by XPS. The survey spectrum (inset in Fig. 3) of 20-CuO/RuO_2 composite shows the distinctive XPS peaks of ruthenium, carbon, oxygen, copper, as well as their auger peaks. Signals of silicon and sodium could hardly be identified, further indicating the complete removal of the silica framework. Fig. 3A focused on the region where the XPS signals of Cu 2p (925–960 eV) in *X*-CuO/RuO_2 (*X* = 10, 20, and 30) catalysts were expected to appear. Accordingly, the Cu $2p_{3/2}$ and Cu $2p_{1/2}$ peaks at around 934 and 954 eV with broadened peak at 940–945 eV in the spectra can be attributed to Cu(II) ions in form of CuO [30,31]. The intensity of the Cu 2p peaks increased with the increase in copper content. It can also be found from Fig. 3A that there is a shoulder peak at about 932.5 eV, which, if compared with literature data [32], seems to be resulted from the Cu(I) ions, indicating that there is a very small amount of Cu(I) ions present in the mesoporous CuO/RuO_2 composite in comparison with the dominant Cu(II) ions. Fig. 3B shows the XPS spectra of Ru 3d obtained from the mesoporous Cu–Ru bimetal oxides. The component with a binding energy of 281 and 285.6 eV can be attributed to the Ru $3d_{5/2}$ and Ru $3d_{3/2}$ in RuO_2, which is consistent with the literature [33].

Fig. 4A gives the N_2 sorption isotherms of the Cu–Ru bimetal oxides. It can be seen clearly that m-RuO_2 and CuO/RuO_2 composites show typical characters of mesoporous transitional-metal oxides replicated via the nanocasting pathway from mesoporous silica [34–36]. This indicates that the mesostructure of RuO_2 or Cu–Ru bimetal oxides has been partially preserved after the removal of silica template. Fig. 3B gives the pore size distribution curves of the samples. Compared to that of silica template in the inset, it could be found that all the CuO/RuO_2 composites showed bimodal pore size distributions in the range of 2–5 and 9–12 nm, which were produced by the removal of silica wall and the textural porosity among the particles, respectively. However, sample m-RuO_2 showed only one distribution peak at about 4.2 nm matching well with the wall thickness of silica template (4.4 nm) as shown in Table 1. Accordingly, the BJH pore size of m-RuO_2 was smaller than that of the Cu–Ru bimetal oxide. The BET surface areas, BJH pore sizes and corresponding pore volumes of the prepared samples were listed in Table 1. All the mesoporous bimetal oxide replicas exhibited relatively large BET-specific surface areas (>90 $m^2\ g^{-1}$). This means that the Cu–Ru bimetal oxides synthesized by co-nanocasting-replication method have the merits of well-maintained large surface areas and pore volumes as well as homogeneous dispersion of components.

3.2. Catalytic performance for NH_3 oxidation

The catalytic activities of the mesoporous CuO/RuO_2 catalysts for ammonia oxidation are shown in Fig. 5A, and the corresponding

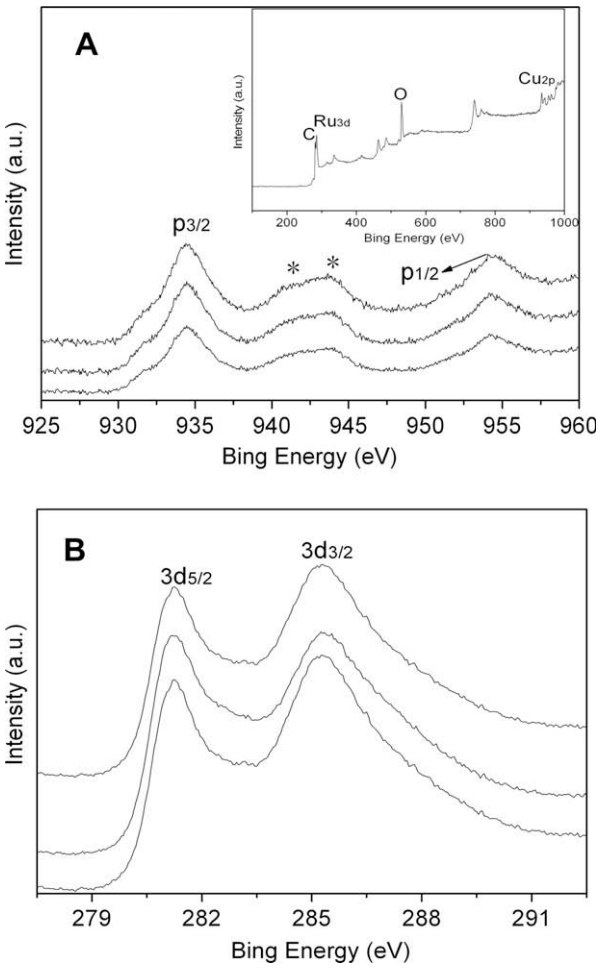

Fig. 3. XPS spectra of core level region of Cu 2p (A) and Ru 3d (B) obtained on mesoporous copper–ruthenium bimetal oxides at copper contents of 10 wt.% (bottom curve), 20 wt.% (middle curve) and 30 wt.% (top curve); inset in (A) is the survey spectrum of 20-CuO/RuO_2.

data are listed in Table 1. The onset reaction temperature of NH_3 oxidation on m-RuO_2 was at 125 °C with the T_{50} at 202 °C. After the CuO addition of limited amounts, the catalytic activity of the bimetal oxides was significantly enhanced, and the reaction of NH_3 oxidation started at 90 °C on 5-CuO/RuO_2 and completed at 200 °C, and the corresponding T_{50} was 153 °C, which were much lower than those on m-RuO_2. Increasing the CuO content, the catalytic activity of bimetal oxide for NH_3 oxidation was further enhanced. T_{50} of sample 10-CuO/RuO_2 was as low as 115 °C, the lowest among all samples, and the complete ammonia conversion temperature on it was at 180 °C, much lower than those (~250 °C) of Cu–Ag catalysts supported on alumina [12] and those (250–300 °C) of V_2O_5/TiO_2 catalysts [21]. The complete ammonia oxidation temperature is one of the important factors to characterize the catalytic activity of catalyst, therefore, the sample 10-CuO/RuO_2 with a complete NH_3 conversion temperature of 180 °C should be a satisfactory catalyst for the low-temperature NH_3 oxidation reaction. However, if the CuO content was increased further, the activity of CuO/RuO_2 bimetal oxides for NH_3 oxidation reaction would decrease gradually, e.g., T_{50} values for samples 15-CuO/RuO_2, 20-CuO/RuO_2 and 30-CuO/RuO_2 were as high as 138, 162 and 175 °C, respectively.

Besides the complete ammonia oxidation temperature, the selectivity of NH_3 oxidation to N_2 should be a widely concerned issue for the ammonia catalytic oxidation. From Fig. 5B, it could be found that the N_2 selectivity of the ammonia oxidation on all the bimetal oxides was 95% and above, and it even reached 100% on

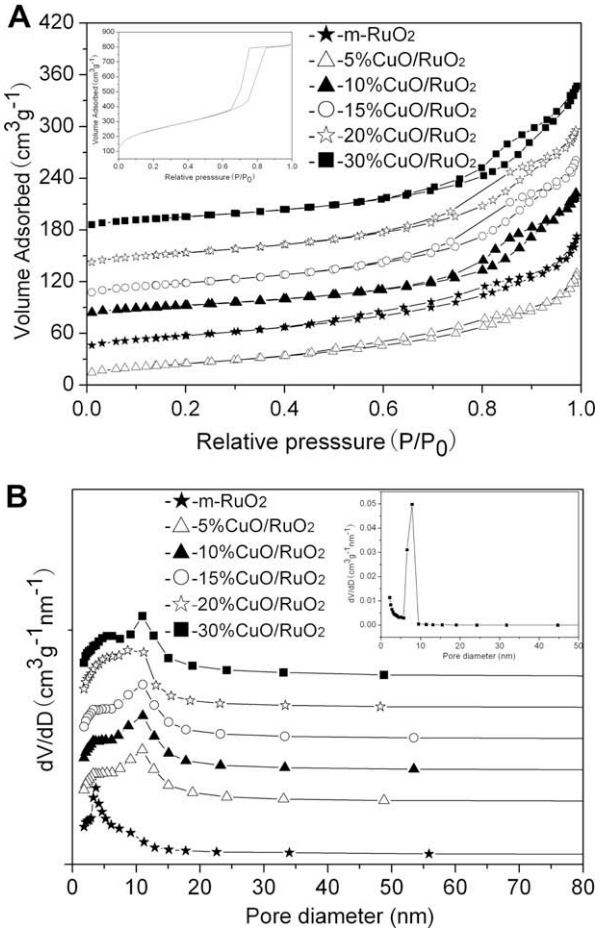

Fig. 4. (A) Nitrogen sorption isotherms of the prepared samples and the mesoporous silica template (KIT-6, inset); (B) the corresponding pore size distribution curves of the replicas and the template (inset).

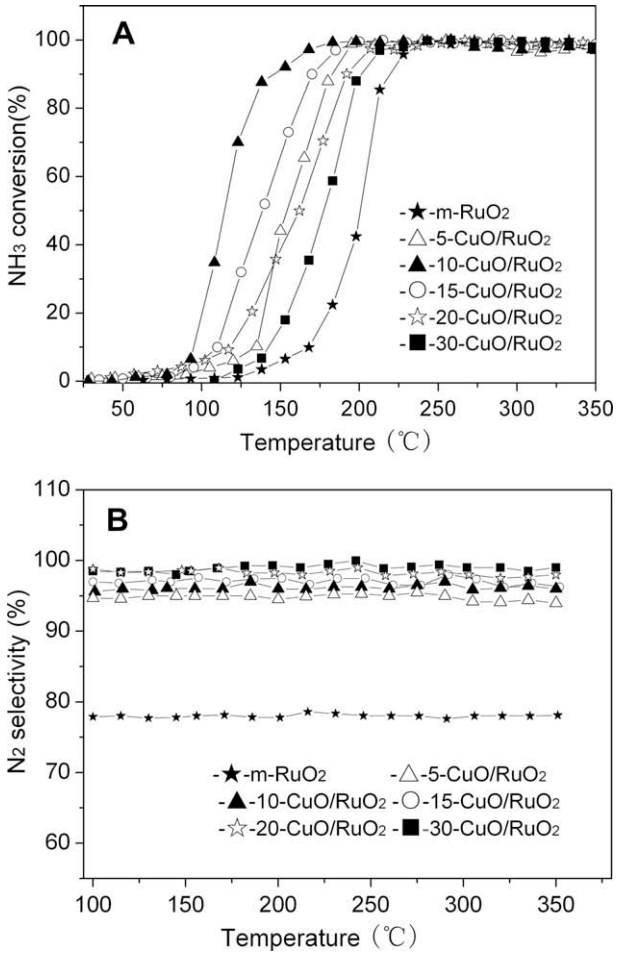

Fig. 5. (A) The NH_3 oxidation conversion rate vs. temperature plots catalyzed by mesoporous RuO_2 and mesostructured CuO/RuO_2 composites; (B) the corresponding selectivity curves of ammonia catalytic oxidation to N_2.

Table 1
Pore structural parameters and the catalytic activities of template and the prepared *X*-CuO/RuO_2 replicas.

Sample	BET surface area ($m^2\ g^{-1}$)	BJH pore size (nm)	Pore volume ($cm^3\ g^{-1}$)	T_{50} (°C)	SCO to N_2 (%)
KIT-6 template	883	6.3	1.31	–	–
m-RuO_2	102	7.1	0.20	202	78
5-CuO/RuO_2	95	8.9	0.19	153	95
10-CuO/RuO_2	98	9.6	0.24	115	97
15-CuO/RuO_2	97	9.0	0.25	138	98
20-CuO/RuO_2	103	8.4	0.27	162	99
30-CuO/RuO_2	98	9.8	0.28	175	100

KIT-6: d_{211} = 9.38 nm, thickness of pore wall = 4.4 nm.

mesostructured 30-CuO/RuO_2 composite significantly higher than that on pure m-RuO_2 (78%), which was desirable for the elimination of ammonia pollution. Moreover, the N_2 selectivity of NH_3 oxidation on the CuO/RuO_2 composites increased with the increase in CuO content. This indicates that the CuO component affects the N_2 selectivity differently from the catalytic conversion for ammonia oxidation. It is proposed that the simultaneous enhancement of both the catalytic activity and N_2 selectivity for ammonia oxidation after incorporating 5–15 wt.% CuO into RuO_2 framework should be resulted from the synergetic catalytic effect between copper and ruthenium oxide. Such a synergetic process will be discussed in the following section.

Fig. 6 gives the complete conversion temperature of ammonia oxidation as a function of the CuO content in bimetal oxide catalysts, and the catalytic activity dependence on CuO concentration can be clearly seen. Compared to pure mesoporous RuO_2, the complete conversion temperature of NH_3 oxidation on mesostructured CuO/RuO_2 composites decreased after small amount of CuO addition, and the lowest temperature of 180 °C was achieved on the 10-CuO/RuO_2 composite for the complete ammonia conversion. However, further increasing the amount of CuO addition resulted in the gradual increase in NH_3 complete conversion temperature, and for samples 20-CuO/RuO_2 and 30-CuO/RuO_2, the complete NH_3 conversion temperatures were 190 and 192 °C, respectively.

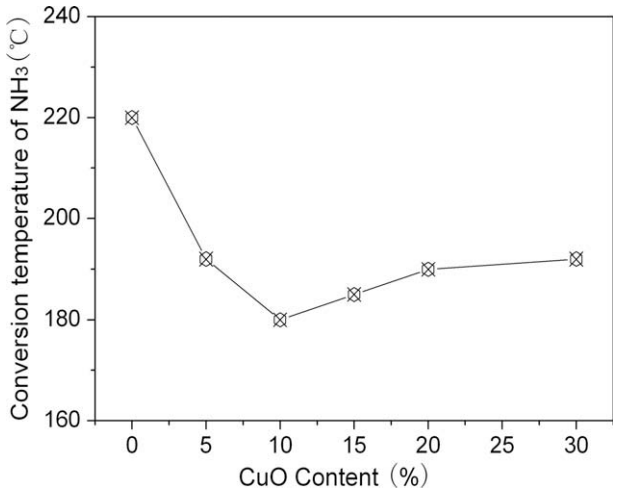

Fig. 6. The complete conversion temperature of NH_3 oxidation vs. CuO content plot for the mesostructured CuO/RuO_2 composite catalysts.

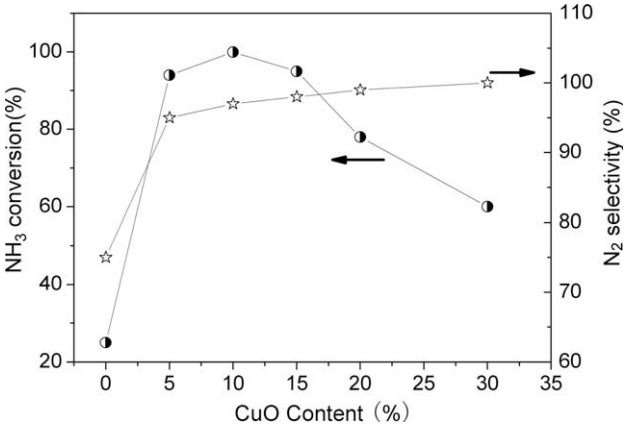

Fig. 7. NH_3 oxidation conversion rate and the corresponding selectivity of NH_3 selective catalytic oxidation to N_2 as a function of CuO content in the mesostructured CuO/RuO_2 composite catalysts at 180 °C.

Under the fixed reaction temperature (180 °C), ammonia conversion rate and the corresponding N_2 selectivity vs. CuO component in CuO/RuO_2 catalysts are shown in Fig. 7. It could be found that the ammonia conversion rate on mesostructured *X*-CuO/RuO_2 (*X* = 0, 5, 10, 15, 20, and 30) catalysts increased remarkably at first with the increase in CuO content and then reached a complete conversion stage at *X* = 10, and it decreased subsequently when *X* > 10. Comparatively, the N_2 selectivity of ammonia oxidation on *X*-CuO/RuO_2 catalysts showed a fast increase at first and then increased gradually with the increase in CuO content. Hundred percent N_2 selectivity could be obtained on 30-CuO/RuO_2 composite, though the ammonia conversion rate for this composite was 60% at 180 °C. These results indicate that CuO plays an important role both in ammonia catalytic oxidation and N_2 selective formation during NH_3 oxidation process.

The enhanced catalytic activity after copper component addition may be ascribed to the synergetic catalytic effect between CuO and RuO_2 during the ammonia oxidation reaction. According to the previous report [37], the (1 1 0) surface of stoichiometric RuO_2 is highly susceptive to NH_3 molecules. This surface possesses numerous dangling bonds and exposes coordinatively unsaturated Ru_{-cus} atoms and therefore is very chemically active. The NH_3 molecules ($NH_{3\text{-}cus}$) and/or oxygen atoms (O_{-cus}) can be adsorbed easily onto these coordinatively unsaturated Ru_{-cus} atoms, as illustrated in Fig. 8A. The interaction between these adsorbed $NH_{3\text{-}cus}$ molecules and O_{-cus} atoms would take place, which leads eventually to the formation of N_{-cus} and H_2O according to report [37] with the following reaction:

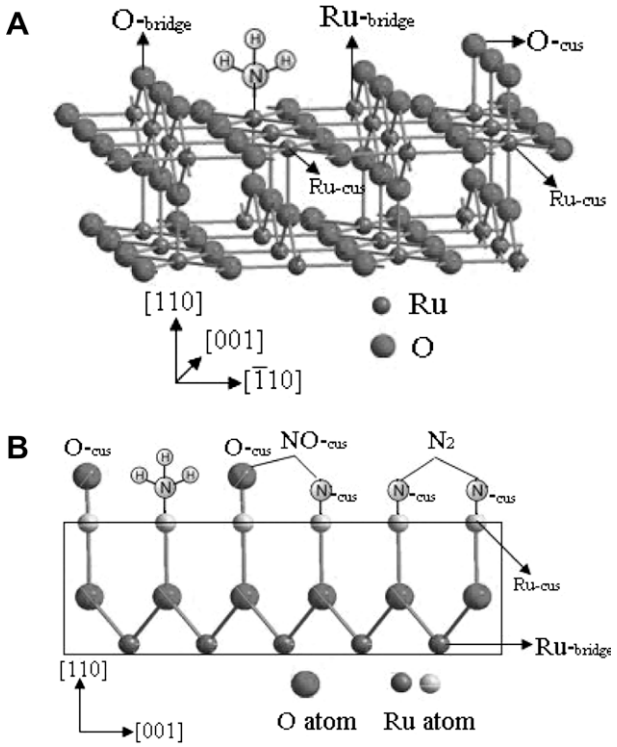

Fig. 8. Schematic drawings of the stoichiometric mesoporous RuO_2 during the SCO of ammonia: (A) stick and ball model of the stoichiometric RuO_2 (1 1 0) surface with adsorbed NH_3 molecules and O atoms (O_{-cus}). O-bridge and Ru_{-cus} are twofold coordinated oxygen atoms and fivefold coordinated Ru atoms, respectively. O_{-cus} is the additional oxygen atom, which may be adsorbed on top of Ru_{-cus} by further exposure to O_2; (B) the possible surface reaction processes and the formation of N_2 between N_{-cus} and N_{-cus}, or NO_x between N_{-cus} and O_{-cus}.

$$NH_{3-cus} + O_{-cus} \rightarrow (NH_2)_{ad} + OH_{ad} \rightarrow N_{-cus} + H_2O \quad (3)$$

The formed N_{-cus} species may recombine either with each other into N_2 or with neighboring O_{-cus} into NO_{-cus}, as shown in Fig. 8B, following reactions (4) and (5), respectively:

$$N_{-cus} + N_{-cus} \rightarrow N_2 \quad (4)$$

$$N_{-cus} + O_{-cus} \rightarrow NO_{-cus} \quad (5)$$

$$NO_{-cus} + NH_{3-cus} \xrightarrow{CuO} N_2 + H_2O \quad (6)$$

On the other hand, CuO is an excellent component, which is active and shows selective catalytic properties in the reduction of NO into N_2 during ammonia oxidation [20,22,23], which means that the NO_{-cus} species adsorbed on the surface of RuO_2 can be reduced to N_2 selectively by CuO following reaction (6). After the reaction following Eq. (6), the active (1 1 0) surface of RuO_2 is exposed again to NH_3 and O_2 molecules, which can be adsorbed onto the surface, making the ammonia further oxidized following Eq. (3). The earlier reaction process following Eqs. (3), (5), and (6), as catalyzed by the mesostructured CuO/RuO_2 catalyst, results in both high conversion of ammonia oxidation and high N_2 selectivity at appropriate content of CuO in the composite, when compared to that on pure mesoporous RuO_2. The content of CuO is an important factor. Over low CuO content (e.g., <5% in the present case) will be not effective enough in enhancing ammonia oxidation activity and N_2 selectivity, however, over high amount of CuO component (e.g., >15% in this case) may cover the active sites on RuO_2 surface to a large extent, leading to the slowing-down of NH_3 adsorption on RuO_2 surface by reaction (3), and consequently the decreased catalytic activity for ammonia conversion. In the meantime, the N_2 selectivity of NH_3 oxidation increases monotonously with the increasing CuO content in the composites following reaction (6), and at higher enough CuO content of 30%, reaction (6) must be fast enough and a 100% N_2 selectivity has been obtained.

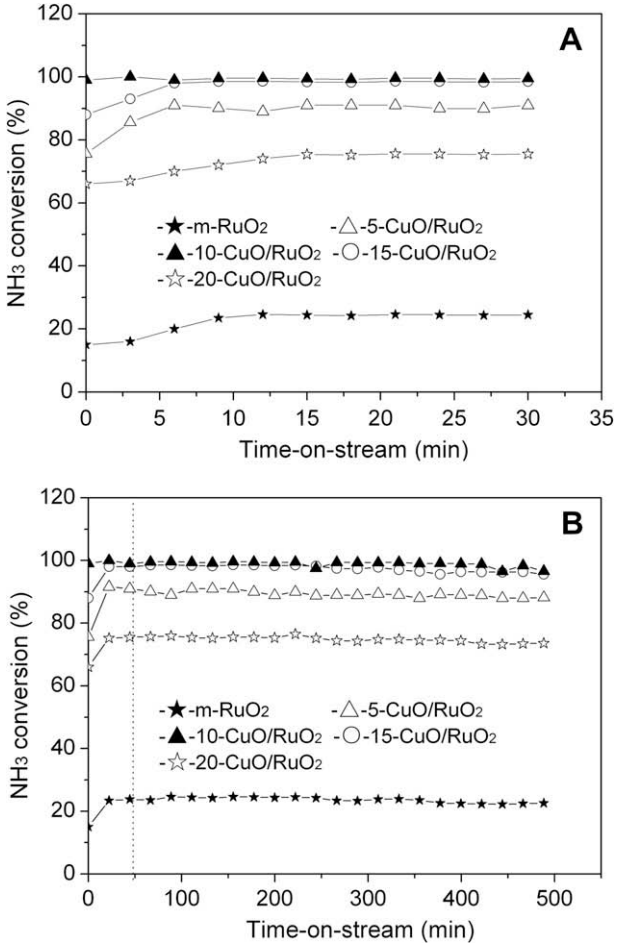

Fig. 9. Time-on-stream behavior of NH_3 oxidation on mesoporous RuO_2 and CuO/RuO_2 composite catalysts at a fixed reaction temperature (180 °C), and (A and B) give the data on different time scales.

Fig. 9 gives the relation between the ammonia oxidation percentage on catalysts and the time-on-stream (TOS) at 180 °C to investigate the catalytic-induction capability and stability of the mesoporous bimetal oxide catalysts of various compositions. The catalytic-induction capability was characterized by the time period needed to achieve a stable conversion for each catalyst at the temperature of 180 °C. For mesoporous m-RuO_2, activation of the catalyst took about 12 min and then reached the steady-state reaction stage according to Fig. 9A. After CuO addition, the activation time became shorter, and it took about 5, 0 and 8 min for 5-CuO/RuO_2, 10-CuO/RuO_2 and 15-CuO/RuO_2, respectively, to reach the steady-state reaction stages under the space velocity (75,000 mL h^{-1} $gcat^{-1}$). As for 20-CuO/RuO_2, the catalyst activation period was prolonged to about 15 min under the same space velocity, which was in accordance with its lower activity. More importantly, it can also be seen from Fig. 9B that each catalyst keeps a stable ammonia conversion rate at the temperature, and no deactivation in ammonia oxidation is observed for as long as 8 h. This reveals the excellent catalytic stability of mesoporous RuO_2 and mesoporous Cu–Ru bimetal oxides toward ammonia oxidation, which is highly desirable as catalysts for the ammonia selective catalytic oxidation process.

4. Conclusions

A co-nanocasting-replication method using *Ia*3*d* symmetry mesoporous silica KIT-6 as hard template has been developed to prepare mesoporous Cu–Ru bimetal oxide catalysts in a wide range of compositions. The mesostructured bimetal oxide replicas exhibited high and stable catalytic activities toward NH_3 oxidation. Addition of an appropriate amount of CuO can significantly enhance the catalytic activity of the mesoporous CuO/RuO_2 composites, and a high N_2 selectivity up to 95–100% can be obtained at the CuO contents >5 wt.% in the composite catalysts. The highest catalytic activity (100% conversion of NH_3 at 180 °C) and a reasonably high N_2 selectivity (97%) have been achieved on the mesostructured CuO/RuO_2 composite catalyst with a CuO content of 10 wt.%. The synergetic catalytic effect between CuO and RuO_2, together with the well-defined mesoporous structure, is believed to be responsible for the achievement of both high catalytic activity toward NH_3 oxidation and high N_2 selectivity on the mesoporous bimetal oxide catalysts. The present mesostructured copper–ruthenium bimetal oxide catalyst should be a promising candidate for the elimination of NH_3 or for the N-containing compounds (NO, NO_2, N_2O).

Acknowledgment

The authors gratefully acknowledge the financial support from National Natural Science Foundation of China with Contracts (20633090, 50872140 and 2007BAJ03B01).

References

[1] M. Amblard, R. Burch, B.W.L. Southward, Appl. Catal. B: Environ. 22 (1999) L159.
[2] M. Amblard, R. Burch, B.W.L. Southward, Catal. Today 59 (2000) 365.
[3] L. Gang, J. van Grondelle, B.G. Anderson, R.A. van Santen, J. Catal. 186 (1999) 100.
[4] R.Q. Long, R.T. Yang, Chem. Commun. 16 (2000) 1651.

[5] R.Q. Long, R.T. Yang, J. Catal. 201 (2001) 145.
[6] A. Akah, C. Cundy, A. Garforth, Appl. Catal. B: Environ. 59 (2005) 221.
[7] G. Olofsson, A. Hinz, A. Anderson, Chem. Eng. Sci. 59 (2004) 4113.
[8] N.I. Il'chenko, Russ. Chem. Rev. 45 (1976) 1119.
[9] P.D. Sobczyk, E.J.M. Hensen, A.M. de Jong, A.S. van Santen, Top. Catal. 23 (2003) 109.
[10] R.Q. Long, R.T. Yang, Catal. Lett. 78 (2002) 353.
[11] J.J. Ostermaier, J.R. Katzer, W.H. Manoque, J. Catal. 41 (1976) 277.
[12] G. Lu, B.G. Anderson, J. van Grondelle, R.A. van Santen, W.J.H. van Gennip, J.W. Niemantsverdriet, P.J. Kooyman, A. Knoester, H.H. Brongersma, J. Catal. 206 (2002) 60.
[13] N. Il'chenko, G.I. Golodets, J. Catal. 39 (1975) 57.
[14] R.Q. Long, R.T. Yang, J. Catal. 207 (2002) 158.
[15] P. Fabrizioli, T. Bürgi, A. Baiker, J. Catal. 206 (2002) 143.
[16] T. Curtin, F. ÓRegan, C. Deconinck, N. Knutte, B.H. Hodnett, Catal. Today 55 (2000) 189.
[17] A. Wöllner, E. Lange, H. Knözinger, Appl. Catal. A: Gen. 94 (1993) 181.
[18] L. Lietti, G. Ramirez, G. Busca, F. Bregani, P. Forzatti, Catal. Today 61 (2000) 187.
[19] L. Chmielarz, P. Kuśtrowski, A. Rafalska-Łasocha, R. Dziembaj, Appl. Catal. B: Environ. 58 (2005) 235.
[20] C.M. Hung, J. Hazard. Mater. 166 (2009) 1314.
[21] Y. Li, J.N. Armor, Appl. Catal. B: Environ. 13 (1997) 131.
[22] G. Lu, J. van Grondelle, B.G. Anderson, R.A. Van Santen, J. Catal. 186 (1999) 100.
[23] C.M. Hung, Powder Technol. 196 (2009) 56.
[24] H.R. Chen, J.L. Gu, J.L. Shi, Z.C. Liu, J.H. Gao, M.L. Ruan, D.S. Yan, Adv. Mater. 17 (2005) 2010.
[25] H.F. Yang, D.Y. Zhao, J. Mater. Chem. 15 (2005) 1217.
[26] A.-H. Lu, F. Schüth, Adv. Mater. 18 (2006) 1793.
[27] D.Y. Zhao, P.D. Yang, B.F. Chmelka, G.D. Stucky, Chem. Mater. 11 (1999) 1174.
[28] X.Z. Cui, Q.J. He, F.M. Cui, J.J. Zhao, L. Li, H.R. Chen, J.L. Shi, Dalton Trans. 18 (2009) 3395.
[29] F. Kleitz, S.H. Choi, R. Ryoo, Chem. Commun. 17 (2003) 2136.
[30] P. Bera, K.R. Priolkar, P.R. Sarode, M.S. Hegde, S. Emura, R. Kumashiro, N.P. Lalla, Chem. Mater. 14 (2002) 3591.
[31] A. Tschöpe, M.L. Trudeau, J.Y. Ying, J. Phys. Chem. B 103 (1999) 8858.
[32] J.F. Moulder, W.F. Stickle, P.E. Sobol, K.D. Bomben, in: J. Chastain (Ed.), Handbook of X-ray Photoelectron Spectroscopy, Perkin–Elmer, Eden Prairie, MI, 1992, p. 231.
[33] H. Mercedes Villullas, F.I. Mattos-Costa, L.O.S. Bulhões, J. Phys. Chem. B 108 (2004) 12898.
[34] F. Jiao, K.M. Shaju, P.G. Bruce, Angew. Chem. Int. Ed. 44 (2005) 6550.
[35] F. Jiao, J.C. Jumas, M. Womes, A.V. Chadwick, A. Harrison, P.G. Bruce, J. Am. Chem. Soc. 128 (2006) 12905.
[36] F. Jiao, A. Harrison, J.C. Jumas, A.V. Chadwick, W.K. Ockelmann, P.G. Bruce, J. Am. Chem. Soc. 128 (2006) 5468.
[37] Y. Wang, K. Jacobi, W.-D. Schölne, G. Ertl, J. Phys. Chem. B 109 (2005) 7883.